High resolution Imaging of Satellites in Daylight

Ryan Swindle
Air Force Research Laboratory (AFRL/RDSM), thomas.swindle@us.af.mil
Douglas Hope
Hart Scientific Consulting International, dhope@hartsci.com
Michael Hart
Hart Scientific Consulting International, mhart@hartsci.com
Stuart Jefferies
Georgia State University, sjefferies@gsu.edu

ABSTRACT

Ground-based imaging of satellites during the daytime represents a formidable challenge due the strong turbulence induced noise in the imagery and the high background noise. Two important approaches for overcoming the problem of imaging through this strong turbulence include aperture partitioning and the collection of wavefront measurements for use in image restoration post-processing. The aperture partitioning enables a reduction in the turbulence induced noise in the recorded imagery, while the wavefront measurements can be used to constrain a frozen flow estimate of the wave front. Together the WFS measurements and FFM enable the recovery of high spatial frequencies in the wave front, which leads to higher fidelity estimates of the PSFs necessary for estimating the recovered image of the satellite. Improvements in image restoration due to the aperture partitioning will be demonstrated by comparing image restoration algorithms that used WFS data with imagery acquired using a filled aperture versus imagery acquired using an aperture partitioning scheme. This comparison will be made using imagery acquired in daylight using a 3m-class telescope.

1 INTRODUCTION

Our recent efforts have focused on implementing the Daylight Object Restoration Algorithm (DORA) [1] at the AMOS site on Mt. Haleakala and Starfire in Albuquerque NM with the goal of obtaining high-resolution imagery using both wave-front sensor (WFS) data and high cadence focal plane imagery. The basis of DORA is the use of a frozen flow model (FFM) of the turbulent layers in the atmosphere, [2] together with the WFS measurements to improve the sampling of the measured wave front, and thus recover high spatial frequencies that are not measured by the WFS. As shown in [1], these high spatial frequency aberrations of the wave-front phase become increasingly damaging to image quality as the seeing worsens, particularly as one moves into the regime of imaging in full daylight. Equivalently, the morphology and fine speckle structure of the PSF are characterized by these the high spatial frequencies, thus their accurate estimation becomes critical to successful image restoration. This loss of information about the high spatial frequencies in strong turbulence regimes greatly limits the capabilities of traditional multi-frame blind deconvolution (MFBD) algorithms in achieving high-resolution imagery. DORA overcomes these limitations through use of the FFM and the WFS data to obtain high-resolution imagery of objects, particularly during full daylight.

2 OBSERVATIONS

On June 8th, 2018, the ENVISAT remote sensing satellite (Norad ID: 27386) was observed in full daylight using the AEOS 3.65m telescope on Mt. Haleakala. Simultaneous WFS and focal imagery were obtained on the target using the DORA-WFS [3] and the ARDI imaging camera [4]. Image data was acquired using both the filled and partitioned aperture observing modes of the ARDI sensor.

A sequence of speckle images of the ENVISAT during full daylight acquired using the full 3.65m aperture of AEOS is shown in Fig. 1. An analysis of the measured tip/tilts yields an estimate for D/r_0 value of 34. This level of turbulence is almost two times above what is typically experienced for twilight observations. In this regime of turbulence, faithful estimation of the high spatial frequencies in the wave front is critical to for achieving a high-resolution image restoration.

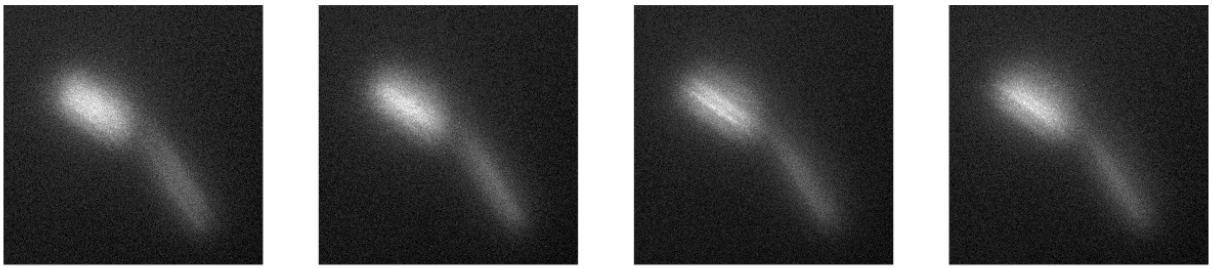

Figure 1 Images of ENVISAT acquired using a filled aperture and an exposure time of 10 msec.

The WFS measurements acquired using the DORA-WFS, can sample using either a 16x16 or 32x32 sampling across the telescope pupil depending on the brightness of the target. For ENVISAT the measurements were made using the 16x16 sampling using an exposure time of 2 msec. An example of a single a WFS image is shown in the left panel of Fig. 2 along with a histogram showing the distribution of the measured slope values.

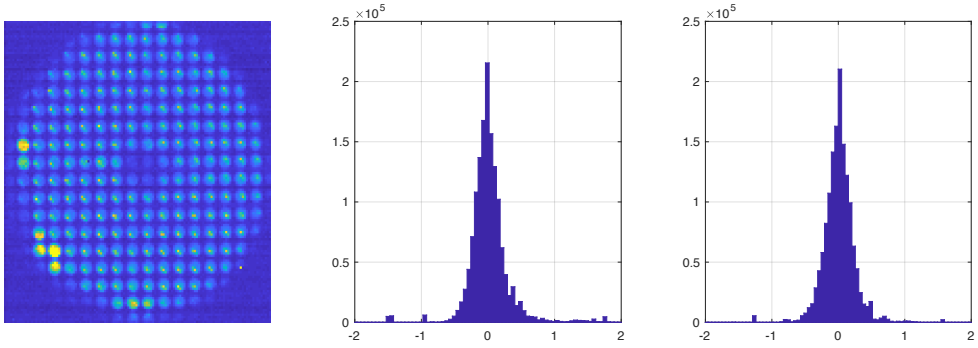

Figure 2 Left panel shows a single WFS image, Panels 2 and 3 shows a histogram of the measured slopes values. Sub-apertures with corrupted slope measurements are evident from the saturated spot image.

The mean measured x/y-gradients are computed and compared to the image x/y-centroids. This enables the WFS data to be correctly associated with the corresponding image frames. Once this synchronization of the WFS and imaging data channels is performed the PSF modeling using a FFM is performed.

Modeling the wave front using a FFM requires knowing the wind velocities of all significant layers of turbulence in the atmosphere. These are computed from an autocorrelation of the WFS measurements, which are captured at a cadence that substantially exceeds the Greenwood frequency and therefore capture the effects of frame-to-frame coherence in the wave front. The calculated wave-front slopes from the DORA-WFS are stacked into a data cube and the 3D spatio-temporal autocorrelation of the cube is calculated. Consider the effect of a wave front characterized by a single frozen layer moving across the pupil. The strongest signal will occur at the center of the autocorrelation cube, at zero spatial and temporal lags. But as time progresses, and the wave front advances across the aperture, the strongest correlation signal will be seen at a spatial lag equal to the elapsed time multiplied by the wind vector. The signature of a frozen layer is thus a line of strong signal projecting from the origin of the autocorrelation cube whose direction corresponds to the direction and speed of the corresponding wind layer. This is shown in Fig. 3 using the measured slopes from the DORA-WFS obtained for the ENVISAT observations. The strength of the correlation signal is directly related to the strength of turbulence in the layer and the rate of decay (1/e folding time) with temporal lag indicates the degree to which the layer is not in fact well represented as a frozen flow. The speed of the two wind layers were 14.1 m/sec for the faster upper layer and 7.96 m/sec for the slower ground layer.

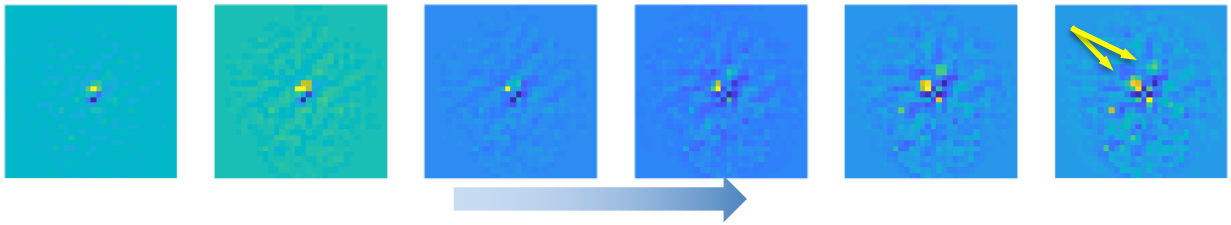

Figure 3 Consecutive time-lag slices from the 3D autocorrelation of the ENVISAT WFS data. Two frozen layers, a strong slow ground layer (moving toward 10 o'clock position) and one fast upper layer (moving toward 1 o'clock position) denoted by the arrows in frame 6.

In WFS observations, the slope value computed at each sub-aperture can become contaminated by noise at different times in the pass. This most likely results from glints from telescope support structures occurring as the telescope slews while tracking the object. These sub-apertures are determined by analyzing the temporal statistics of the computed wave-front slopes and flagging sub-apertures where the computed slopes do not match the expected statistics of the measurements, i.e. zero mean Gaussian variates (see right two panels in Fig. 2).

As the high-resolution wave front is computed using a frozen flow model, a dynamically weighted sub-aperture mask is updated and refined. Any sub-apertures with persistently high residuals are masked out. The sub-aperture mask is iteratively updated until the residuals of the model, and measured slopes, become uniform.

3 RESULTS

The pupil wave front $\Phi(x,t+\Delta t)$ is modeled as a sum of independent static turbulent layers:

$$\Phi(x,t+\Delta t)=\sum\nolimits_i \alpha_i(x-v_i\Delta t,t),$$

where v_i denotes the velocity of the i^{th} layer. For the ENVISAT restorations two wind layers were used build the FFM. The use of the FFM results in better sampling of the high-spatial frequencies of the wave front as clearly shown in Figure 4 where a sequence of wave-fronts reconstructed using only the WFS data (low resolution - top row) and the WFS data + FFM (high resolution - bottom row) are displayed. The high spatial frequencies resulting from use of the FFM, which are clearly evident, are crucial for obtaining a high fidelity model of the atmospheric PSF.

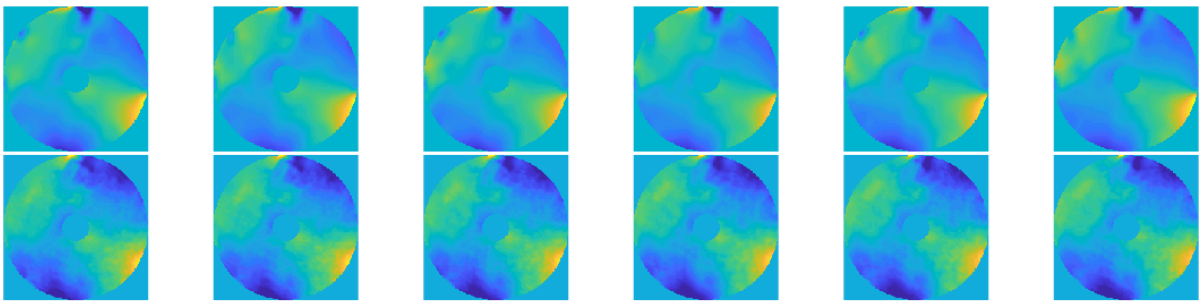

Figure 4 A sequence of wave fronts. Top row: Low-resolution wave fronts made directly from the WFS measurements. Bottom row: High-resolution wave fronts made using WFS measurements with a FFM.

The importance of the high spatial frequencies in the wave-front when performing image restoration is evident by the striking visual improvement in the DORA image restoration in Fig. 5 (third panel) when compared to MFBD using image plane data only (panel one), and MFBD + WFS data. Importantly, this demonstrates that even when WFS data is acquired simultaneously with the imagery [7], this data alone is insufficient to achieve high-resolution imagery using a myopic deconvolution algorithm. This is a consequence of the limited frequency sampling of the wave-front, in the case of ENVISAT a 16x16 sampling at $D/r_0=34$, and stresses the need for DORA when imaging in such strong turbulence regimes. Here r_0 is computed from the variance of the reconstructed high-resolution phases, and is equal to 6 cm at 0.5 μm. This is commensurate with seeing conditions during daylight, as the observations occurred 2.5 hours after sunrise on June 8th (5:44 am)

FFM is crucial for extracting the high spatial frequencies in that wave front that are not sampled by the WFS.

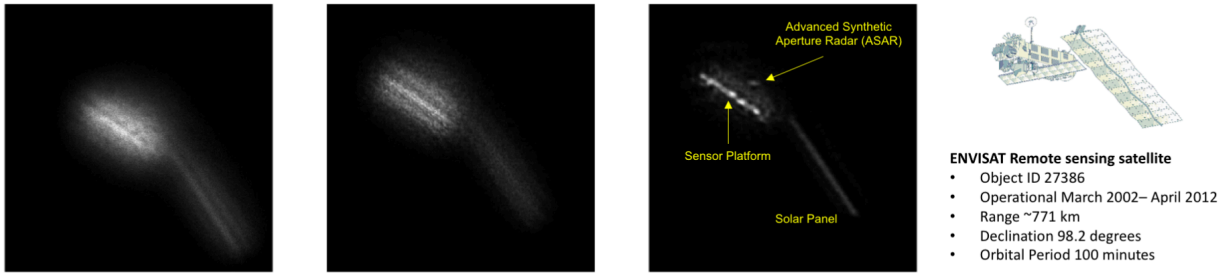

Figure 5 Left: MFBD restoration using image plane data, Center: MFBD restoration using WFS data and Right: DORA MFBD-FFM restoration.

The use of Aperture partitioning in the strong turbulence regimes has been demonstrated [9,10]. An analysis of the ENIVSAT filled aperture and partitioned aperture will be addressed in the near future. Here, DORA will perform a joint estimation using sing the 4-channels where each channel corresponds to an annulus as measured by the ARDI sensor.

4 CONCLUSIONS

DORA restoration capability has been demonstrated using daylight imagery using the DORA-WFS and the ARDI imager. The validity of FFM as a technique for estimating high spatial frequencies in the wave-front, that are not measured by the WFS provides a crucial information required to obtain high resolution imagery when observing satellites in full daylight.

5 ACKNOWLEDGEMENTS

This work has been supported by the Air Force Research Laboratory, Directed Energy Directorate, under contract FA9451-12-C-0004.

6 REFERENCES

[1] D. A. Hope, M. Hart, S.M. Jefferies and J. Nagy, "Myopic Deconvolution from Wave Front Sensing for Images Acquired with Large Spectral and Temporal Bandwidth, AMOS Technical Conference, Kihei, HI, (2013).

[2] Jefferies, S. M. and Hart, M, “Deconvolution from wave front sensing using the frozen flow hypothesis”, Optics Express, 19, 1975-1984 (2011).

[3] M. Hart, S.M. Jefferies, D.A. Hope, J. Nagy, O. Durney, R. Codona, "Quantitative measurements of daytime near infrared sky brightness at the AEOS 3.6 m telescope", AMOS Technical Conference, Kihei, HI, (2014).

[4] S. Griffin, B. Calef, J. Lucas, R. Swindle, L. Schatz, " Aperture Partitioning Element Results," AMOS Technical Conference, Kihei, HI, (2017).

[5] D. A. Hope, M. Hart, S.M. Jefferies and J. Nagy, "Myopic Deconvolution from Wave Front Sensing for Images Acquired with Large Spectral and Temporal Bandwidth, AMOS Technical Conference, Kihei, HI, (2013).

[6] Hart, M. et al., “Multi-Frame blind deconvolution for imaging in daylight and strong turbulence conditions,” Proc. SPIE 8165, 81650L, (2011).

[7] W. Bradford, "Maui4: a 24 hour Haleakala turbulence profile," AMOS Technical Conference, Kihei, HI, (2010).

[8] Charles L. Matson, Kathy Borelli, Stuart Jefferies, Charles C. Beckner, Jr., E. Keith Hege, and Michael Lloyd-Hart, "Fast and optimal multiframe blind deconvolution algorithm for high-resolution ground-based imaging of space objects," Appl. Opt. 48, A75-A92 (2009)

[9] Douglas A. Hope, Stuart M. Jefferies, Michael Hart, and James G. Nagy, "High-resolution speckle imaging through strong atmospheric turbulence," Opt. Express 24, 12116-12129 (2016)

[10] B. Calef, “Speckle imaging with a partitioned aperture: experimental results,” AMOS Technical Conference, Kihei, HI, (2013).
[11] Jefferies, S. M., Hope, D. A., Hart, M., and Nagy, J. G., “High-resolution imaging through strong atmospheric turbulence and over wide fields-of-view,” AMOS Technical Conference, Kihei, HI, (2013).